REPORT DOCUMENTATION PAGE

Form Approved
OMB No. 0704-0188

AD-A233 120

2. Report Date.	3. Report Type and Dates Covered.
1991	Journal Article

4. Title and Subtitle.
Physical Properties and Microstructural Response of Sediments to Accretion-Subduction: Barbados Forearc

5. Funding Numbers.
61153N
Program Element No.
03205
Project No.
330
Task No.
DN257003
Accession No.

6. Author(s).
Elliott Taylor, Patti J. Burkett, Jeri D. Wackler, and John N. Leonard

7. Performing Organization Name(s) and Address(es).
Naval Oceanographic and Atmospheric Research Laboratory*
Ocean Science Directorate
Stennis Space Center, MS 39529-5004

8. Performing Organization Report Number.
JA 360:008:90

9. Sponsoring/Monitoring Agency Name(s) and Address(es).
Naval Oceanographic and Atmospheric Research Laboratory*
Ocean Science Directorate
Stennis Space Center, MS 39529-5004

10. Sponsoring/Monitoring Agency Report Number.
JA 360:008:90

11. Supplementary Notes.
*Formerly Naval Ocean Research and Development Activity
MFGS

12a. Distribution/Availability Statement.
Approved for public release; distribution is unlimited.

12b. Distribution Code.

13. Abstract *(Maximum 200 words).*
Convergent margins are one of three major geological boundaries in terms of relative plate motion. These margins are sites where large piles of sediment are being physically transferred from one tectonic plate to another, often forming the roots of extensive mountain systems. Important global fluid and mass fluxes take place at these locations. The Barbados Ridge represents the growing pile resulting from sediment being scraped off the Atlantic plate and added to the Caribbean plate (Fig. 22.1). This transfer process results in accretion through lateral shortening and vertical thickening of the sediment package. Some of the sediment pile on the Atlantic plate is not initially offscraped. A major detachment fault, or decollement, separates material being accreted from that being subducted. Samples from this region were taken to determine the structural and physical changes associated with sediments undergoing accretion or subduction, and to understand the features that control the location of the slip plane, or decollement, between these two units.

14. Subject Terms.
(U) Sediment Transport; (U) Sediments; (U) Pore Pressure; (U) Clay

15. Number of Pages.
16

16. Price Code.

17. Security Classification of Report.	18. Security Classification of This Page.	19. Security Classification of Abstract.	20. Limitation of Abstract.
Unclassified	Unclassified	Unclassified	SAR

Reprinted from

Richard H. Bennett, William R. Bryant, and Matthew H. Hulbert
Editors

Microstructure of Fine-Grained Sediments

Springer-Verlag
New York Berlin Heidelberg London
Paris Tokyo Hong Kong Barcelona

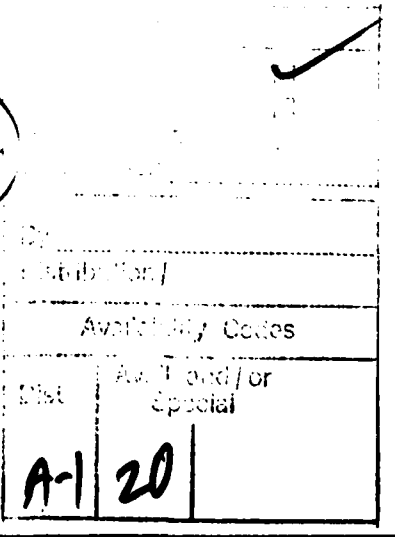

CHAPTER 22

Physical Properties and Microstructural Response of Sediments to Accretion–Subduction: Barbados Forearc

Elliott Taylor, Patti J. Burkett, Jeri D. Wackler, and John N. Leonard

Introduction

Convergent margins are one of three major geological boundaries in terms of relative plate motion. These margins are sites where large piles of sediment are being physically transferred from one tectonic plate to another, often forming the roots of extensive mountain systems. Important global fluid and mass fluxes take place at these locations. The Barbados Ridge represents the growing pile resulting from sediment being scraped off the Atlantic plate and added to the Caribbean plate (Fig. 22.1). This transfer process results in accretion through lateral shortening and vertical thickening of the sediment package. Some of the sediment pile on the Atlantic plate is not initially offscraped. A major detachment fault, or decollement, separates material being accreted from that being subducted. Samples from this region were taken to determine the structural and physical changes associated with sediments undergoing accretion or subduction, and to understand the features that control the location of the slip plane, or decollement, between these two units.

Understanding sediment deformation and related physical changes at convergent margins has been the motive behind several Deep Sea Drilling Project (DSDP) and Ocean Drilling Program (ODP) coring programs. Sediment fabrics resulting from deformation during the accretion process are wide ranging and have been documented on scales varying from meters to microns. Small-scale visible structures include veins, scaly fabrics, scaly cleavage, folding, and faulting (Lundberg and Moore, 1986). Sediment physical properties may undergo significant to little change in these tectonically active areas, as described for the Barbados Forearc (Marlow et al., 1984), Middle America Trench (Shephard et al., 1982; Taylor and Bryant, 1985), Peru Trench (Suess et al., 1988), Cascadia margin (Carson, 1977), Aleutian Trench (Lee et al., 1973), Japan Trench (Carson and Bruns, 1980; Shephard and Bryant, 1980), and Nankai Trough (Bray and Karig, 1985, 1986; Johns, 1986). The relationship between the variability of physical change and related structural and tectonic features of these margins has been suggested through studies such as Carson et al. (1982), Shephard and Bryant (1983), and Carson and Berglund (1986). Cowan et al. (1984) described the development of strong, planar, preferred orientation in clayey mud related to a major thrust fault cored at the Barbados forearc. Chiou (1981) and Shephard et al. (1980) discussed some aspects of sediment microfabric reorientation and development of a preferred fabric direction in fine-grained sediments from the Middle America Trench. Knipe (1986) provided detailed scanning electron microscopy (SEM) and transmission electron microscopy (TEM) images of vein-related microfabric in Japan Trench sediments.

The Barbados convergent margin was cored during DSDP Leg 78A (Biju-Duval et al., 1984) and ODP Leg 110 (Mascle et al., 1988). Both cruises provided material from the Barbados forearc to study the process of offscraping and subduction. The Leg 110 coring program drilled at six sites located along a 22-km-long transect perpendicular to the deformation front (Fig. 22.1). In this chapter we focus on results from Leg 110 Sites 672 and 671. Site 671 penetrated 691 m below sea floor (mbsf), in 4932 m water depth, recovering cores from the offscraped accretionary prism and sediments being subducted below the decollement. Site 672, drilled 6 km seaward of the deformation front in 4982 m water depth, sampled 494 m of the sediment section resting on the Atlantic plate. In this study we document the microstructural changes in sediments in context of the observed physical properties, with emphasis on subcentimeter-scale features observed in X-radiography, SEM, and TEM.

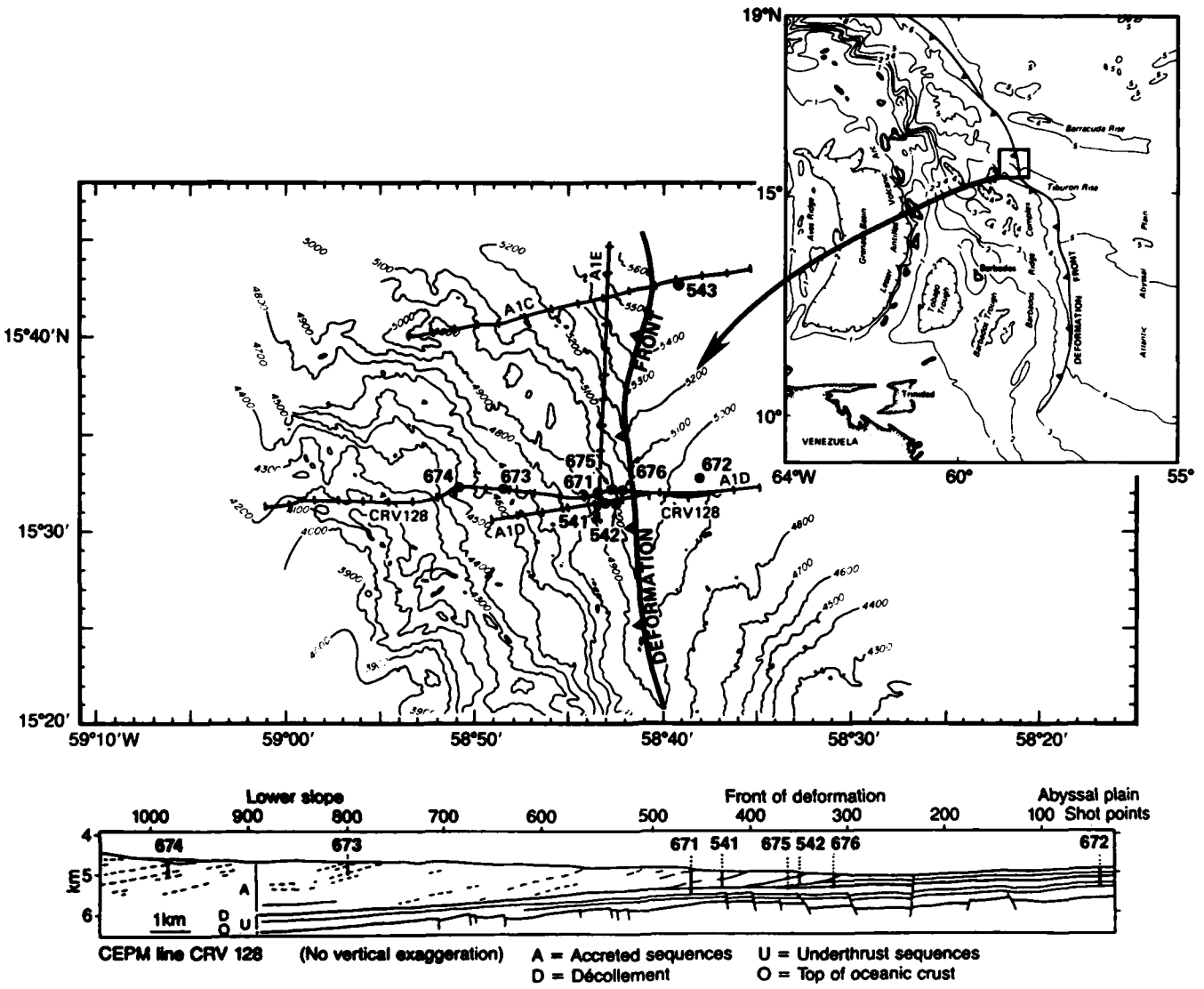

Figure 22.1. Location of Leg 110 drill sites across the Barbados Ridge.

Methods

Shipboard analyses of physical properties included index properties, GRAPE (indirect measure of bulk density through gamma-ray transmission), compressional wave velocity, vane shear strength, and thermal conductivity (Mascle et al., 1988). Shore-based studies covered both geotechnical and structural studies. Geotechnical testing included uniaxial consolidation (oedometer) tests (D2435 in ASTM, 1981; Lowe et al., 1964) and permeability (Lambe, 1951). Geotechnical samples were obtained to depths limited by sediment induration (approximately 200 mbsf at Sites 671 and 672).

Consolidation results are expressed as overconsolidation difference (OCD):

$$\text{OCD} = P'_c - P'_o$$

where P'_c is the preconsolidation stress and P'_o the effective overburden stress (Lambe, 1969). Permeabilities are expressed in terms of hydraulic conductivity. Values reported herein are interpolated for expected *in situ* void ratios and viscosity corrected to *in situ* temperatures using thermal gradients reported in Mascle et al. (1988).

Structural studies of the ODP Leg 110 cores include visual core descriptions complemented with shore-based X-radiographs, SEM, and TEM analyses. Samples for shore-based studies were selected to obtain the best coverage of major structural elements in the convergence process: offscraped, decollement, and underthrust sediments. Attempts were made to choose samples near

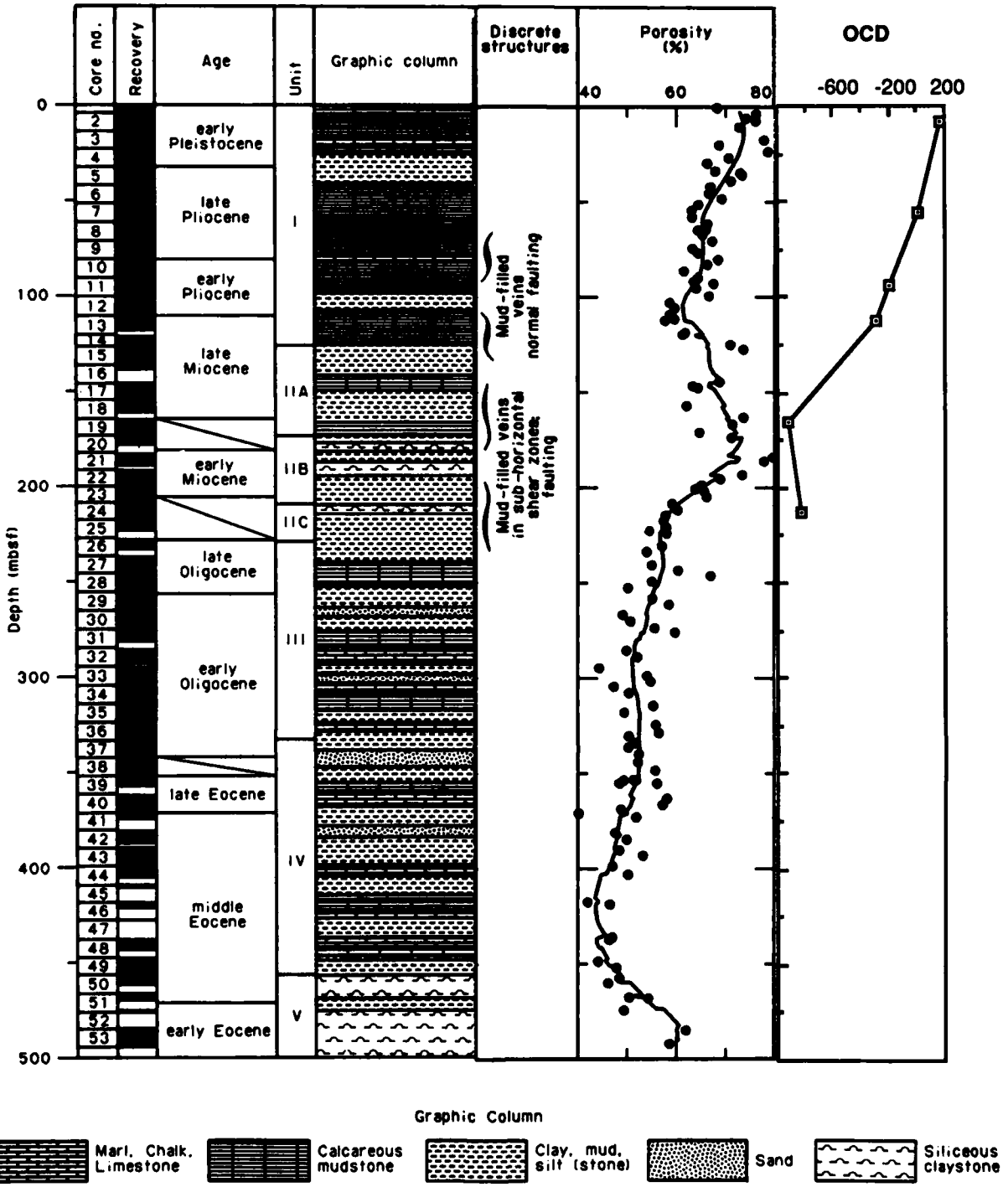

Figure 22.2. Lithology, structural features, porosity, and OCD of Site 672 sediments. Shallow overconsolidated sediments appear to be progressively underconsolidated with increasing depth.

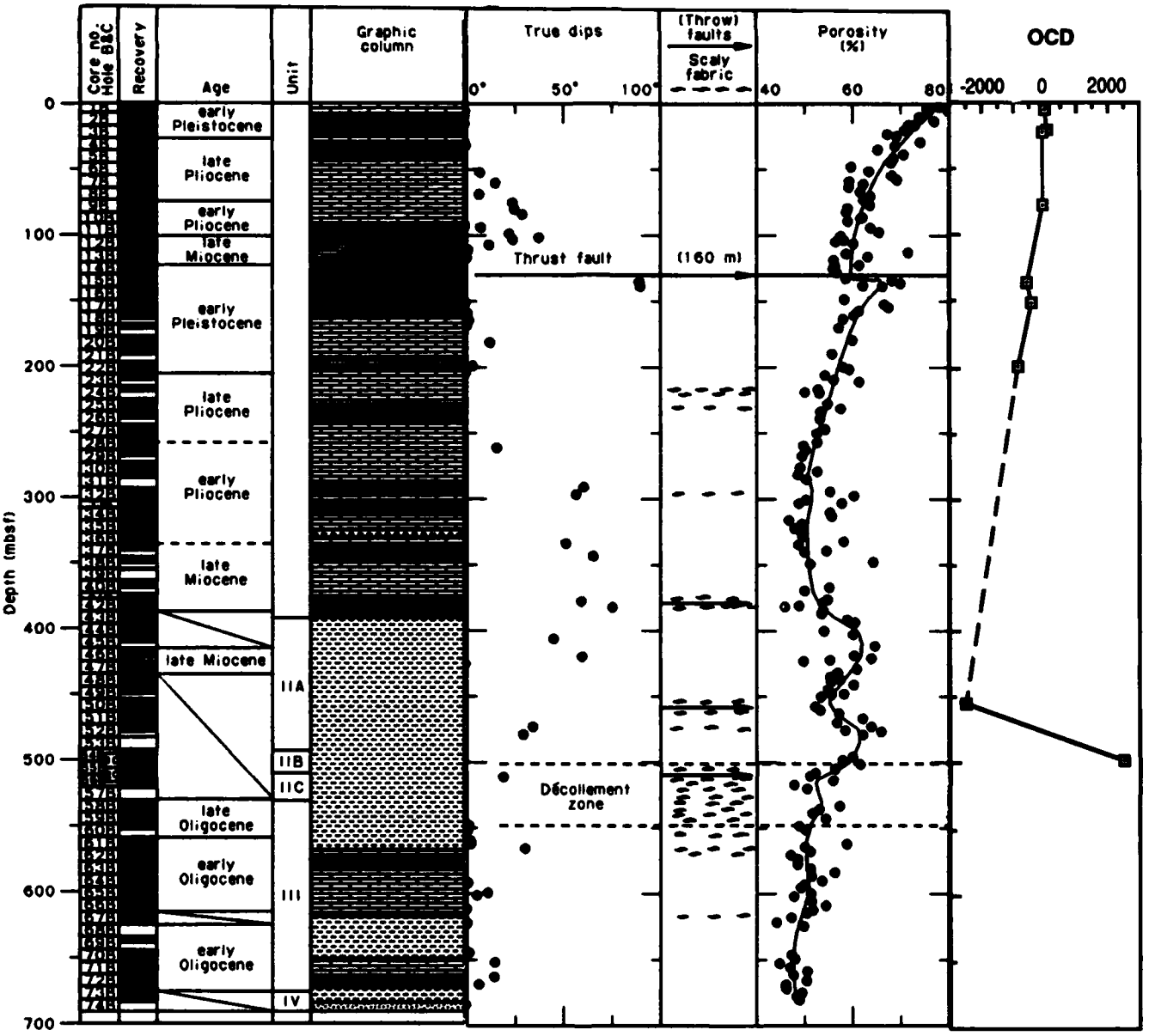

Figure 22.3. Lithology, structure features, porosity, and OCD of Site 671 sediments. The apparent underconsolidation of accreted sediments is strongly contrasted by the high OCD within the decollement (see Fig. 22.2 for key to symbols).

those for geotechnical analyses and from sites nearest the deformation front: Sites 671, 676, and 672.

X-Radiographic studies were carried out on selected 1-cm-thick slabs of core to obtain optimum resolution. Stereo pair X-radiographs were prepared to enhance structural interpretation. Exposures were obtained using methods described in Wackler (1988).

SEM and TEM samples were oriented blocks prepared for sputter coating (SEM) or epoxy impregnation (TEM) through critical point drying (Chiou, 1981; Burkett, 1987; Burkett et al., this volume). Most SEM samples were scanned at 15, 100–200, 450, and in cases at 1000× magnifications. TEM photomosaics were prepared to provide fine-scale coverage of six samples from Hole 671B. Hence, TEM samples represent material only from the offscraped sediment pile.

Sediment Physical Properties

The changes affecting the sediment column during convergence may be reflected in alterations of physical and geotechnical

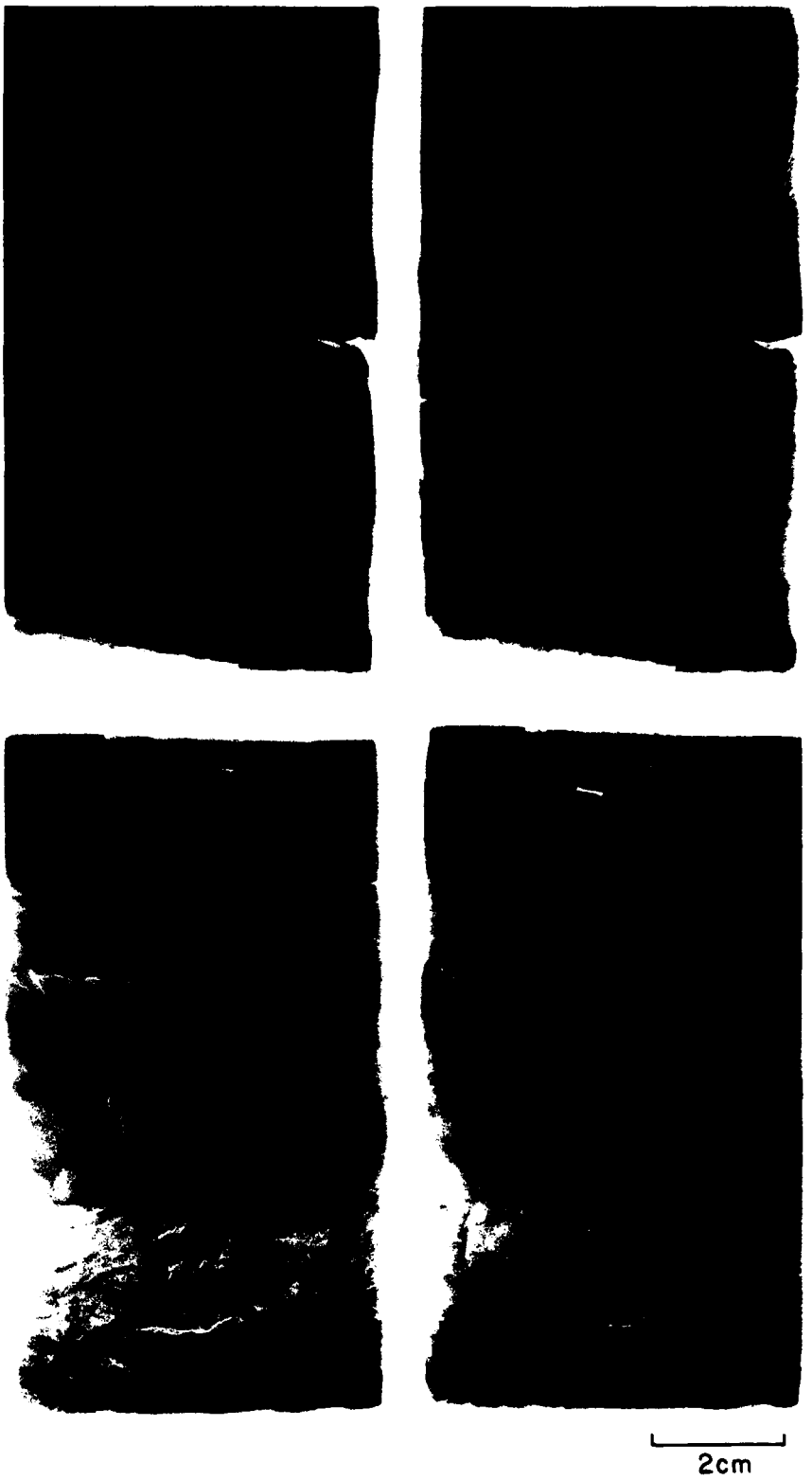

Figure 22.4. Stereopair X-radiographs of millimeter-scale structural deformation in Barbados Ridge sediments. Top: Sample 672A-28X-3. Faint bidirectional faults with dips near 20° are located in the upper half (A). The large fracture in the middle is drilling induced (B). The light dendritic pattern at the top is interpreted as incipient dewatering structures (C). Bottom: Sample 671B-55X-5. Examples of microscopic subhorizontal scaly fabric are indicated by arrows.

Figure 22.5(a–c). TEM photograph mosaics of Sample 671B-2H-2 (8.9 mbsf). Porosity: 76%. This unoriented sample exhibits an open structure of randomly oriented domains (M, matrix) surrounding biogenic particles (B), such as foraminiferal tests and nannofossils, and fractillites (F). Possible dewatering paths are indicated by channels (C) and by pore spaces with face-to-face arranged particles forming a rim around the pathway (W).

properties. Comparison of sediment characteristics from the seaward Site 672 with those of Site 671 in the prism provides an overview of the changes in the immediate vicinity of the deformation front. Site 672, drilled 6 km east of any evidence of convergence in seismic profiles, was intended to provide reference material against which sediments from within the arc could be compared. Structurally disrupted sediments and evidence of significant fluid flow within the cored section, however, suggest this site does not adequately serve as a reference (Mascle et al., 1988). Nevertheless, contrasting sediment properties between Sites 671 and 672 serve to illustrate the scale of structural and physical modification taking place during early convergence.

Site 672

The porosity versus depth profile of Site 672 sediments shows a pattern consistent with most marine sediments. A sharp decrease in porosity near surface proceeds downhole to a gentler gradient (Fig. 22.2). Superimposed on Site 672 is the porosity–depth function defined for terrigenous sediments (Hamilton, 1976). A clear departure for this trend occurs at about 120 mbsf, corresponding to a lithologic change from calcareous oozes/mud above to the smectitic and radiolarian mud(stone) of Unit 2 below. Maximum porosities of 78% occur at the top of the radiolarian-rich Subunit IIb and decrease sharply within Subunit IIc. Sediment composition appears to exert a major control on the physical properties at this site.

Geotechnical test results indicate near-surface sediments are overconsolidated above 7 mbsf, normally consolidated to about 50 mbsf, and underconsolidated below that depth (Fig. 22.2). Maximum apparent underconsolidation occurs near the future, or propagating, decollement within Subunit IIb. This underconsolidated state may be a result of low effective stress within the sediment column arising from excess *in situ* pore pressures at those depths. Below the propagating decollement, sediments are

Figure 22.5. (b)

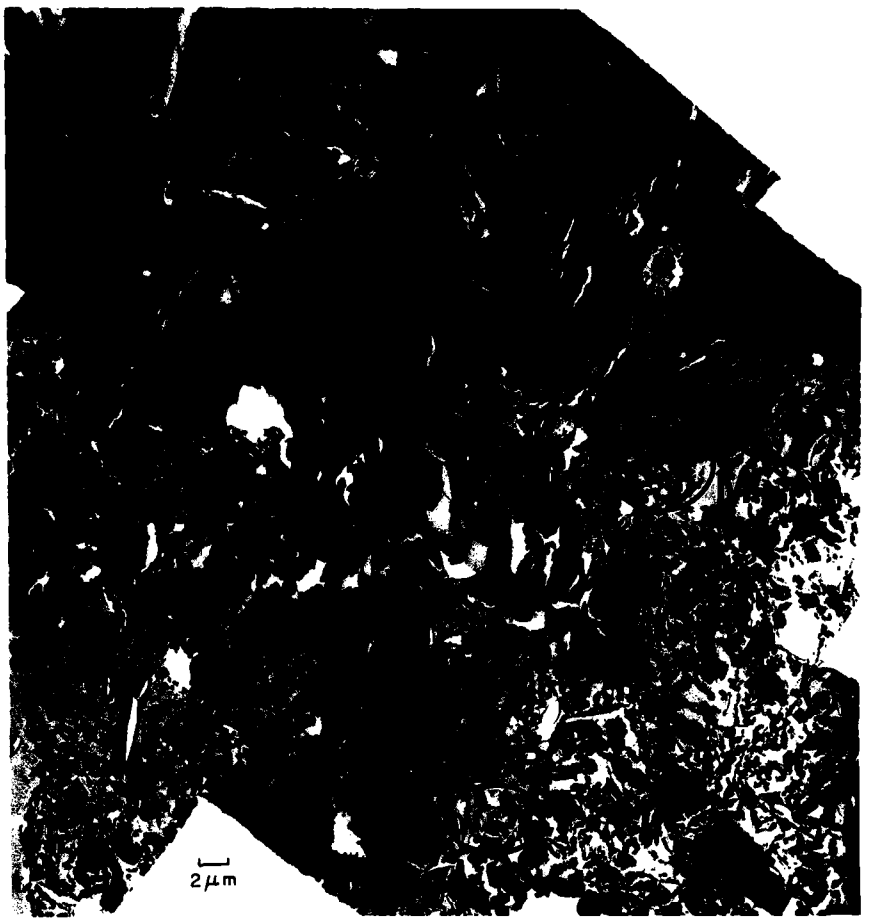

underconsolidated to the extent of those immediately above that major slip plane, thus disrupting the downhole trend of increasing underconsolidated behavior.

Permeabilities vary from about 10^{-6} to 10^{-8} cm/sec within the upper 200 m. These values are typical of hemipelagic sediments under similar burial depths (Bryant et al., 1981).

Site 671

The nearly 700-m-deep hole cored at this site sampled offscraped and underthrust sediment, coring through the decollement at 500–540 mbsf. Several thrust faults cut through the offscraped sediment section at this site, resulting in structural repetition of stratigraphic units (Fig. 22.3). Sediments in the uppermost 120 m exhibit a porosity–depth function similar to sediments at Site 672. A major thrust fault at 128 mbsf is evident in the nonuniform porosity profile. Below that depth, porosity decreases nonlinearly to near 200 mbsf where it resumes a fairly linear decrease with depth. Sediment composition, as at Site 672, strongly influences the index properties at Site 671. The repetition of porosity maxima at 410 and 475 mbsf is attributed to a probable thrust fault between these two depths. The decollement, stratigraphically located within a lower Miocene siliceous mudstone interval, is marked by an abrupt change in porosity. Values decrease from about 60 to 47% over the 40-m-thick interval.

Geotechnical results of Site 671 samples are similar to those obtained for Site 672. The OCD values are more negative with depth in the offscraped sequence. Maximum underconsolidation is probably located immediately overlying the decollement and, as at Site 672, may reflect lower effective overburden stress resulting from higher pore pressures at those depths. The distinct shift of the OCD within the decollement suggests sediments are effectively consolidating, probably as a result of shear-imposed deformation and/or the proximity to effective dewatering paths through more permeable fractured mudstone.

Permeabilities within Site 671 sediments are directly related to the porosity trends. The range of 10^{-7} to 10^{-9} cm/sec is slightly lower than that of Site 672. At comparable depths, Site 671 permeabilities are almost half an order of magnitude less than those of Site 672. This decrease across the arc, like porosity, indicates lateral consolidation is taking place within the accreted package.

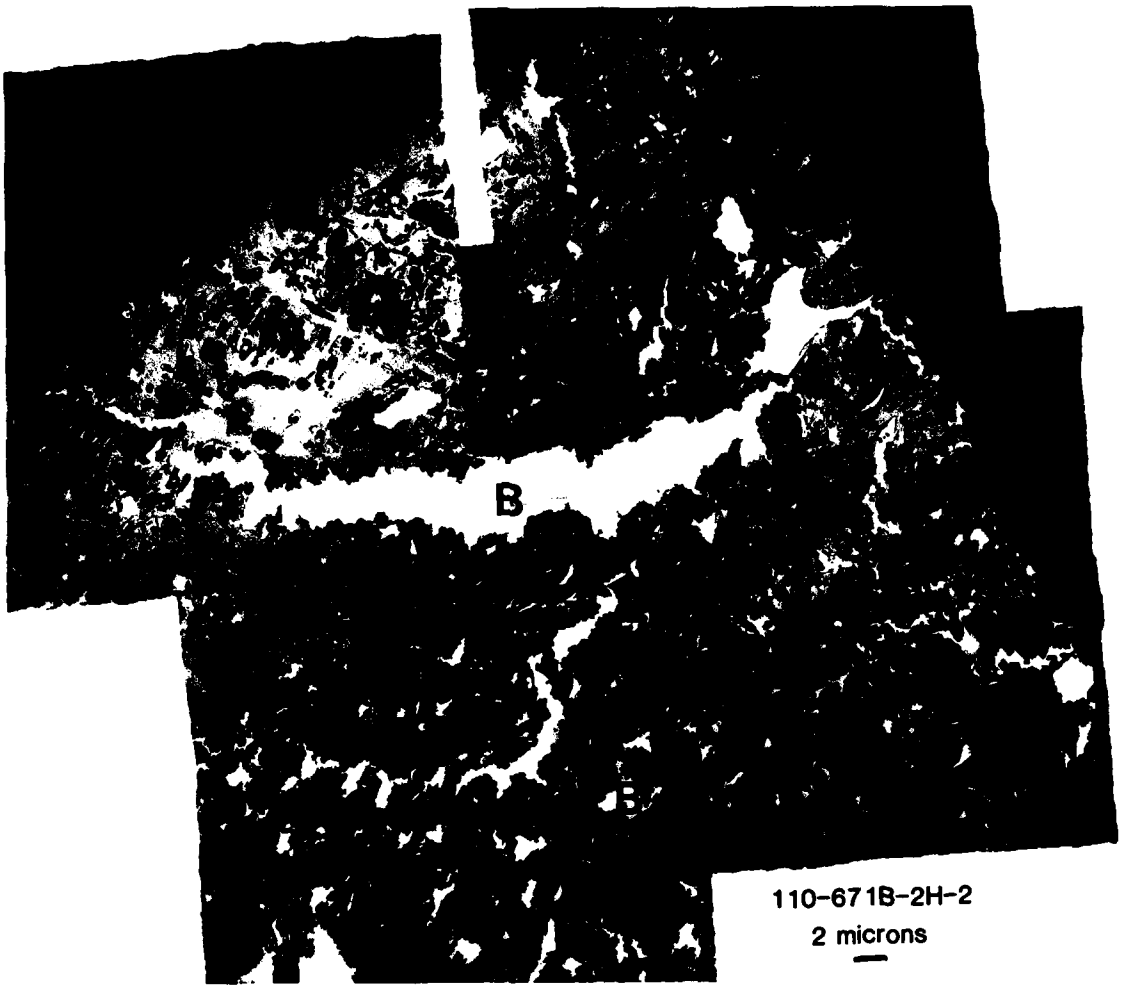

Figure 22.5. (c)

Sediment Macrostructural Features

Structural evidence of the convergent process is observable in sediments from both Sites 671 and 672. The decollement at Site 671 is perhaps the principal structural feature, characterized by oxidized, Mn-stained, siliceous mudstone with a pervasively subhorizontal scaly fabric. Evidence of fluid migration through scaly fabric is found in localized calcite or rhodochrosite-filled veins. Similar features are also described for sediments at Site 672, casting doubt on its usefulness as a "reference" site.

Zones of scaly fabric are found at both Sites 671 and 672, and not always associated with thrust faults. Scaly fabric and dewatering veins are characteristic of sediments overlying the decollement, whereas underthrust sediments appear undeformed or exhibit brittle cleavage. Other sites cored during Leg 110 also show sediments are progressively deformed as they are further incorporated into the accretionary wedge.

X-Radiography of select sediments serves to closely examine structural features on centimeter to millimeter scales. Wackler (1988) documented incipient development of scaly fabric, slickensided microthrusts, microfolding, and submillimeter dendritic patterns possibly reflecting fluid-escape structures (Fig. 22.4).

Sediment Microfabric

SEM and TEM photographs of selected samples from Site 671 were made to document fabric modification in accretion and subduction. The uppermost sediments have an open fabric of fine-grained sediments interspersed with silt- to sand-sized foraminifer tests and fractillites (fractured illites; Bryant and Bennett, 1988) (Fig. 22.5). The foraminiferal tests help maintain a high porosity in these sediments. Dewatering channels, rimmed by locally aligned domains, appear throughout these uppermost sediments. The edge-to-edge and edge-to-face clay particle arrangements in the shallow sediments of Hole 671B become progressively more oriented downhole, forming domains of face-to-face clay packets (Fig. 22.6). Core 671B-8H-4 exhibits numerous fractillites in TEM, and development of preferred subhorizontal alignment in localized fine-grained matrices.

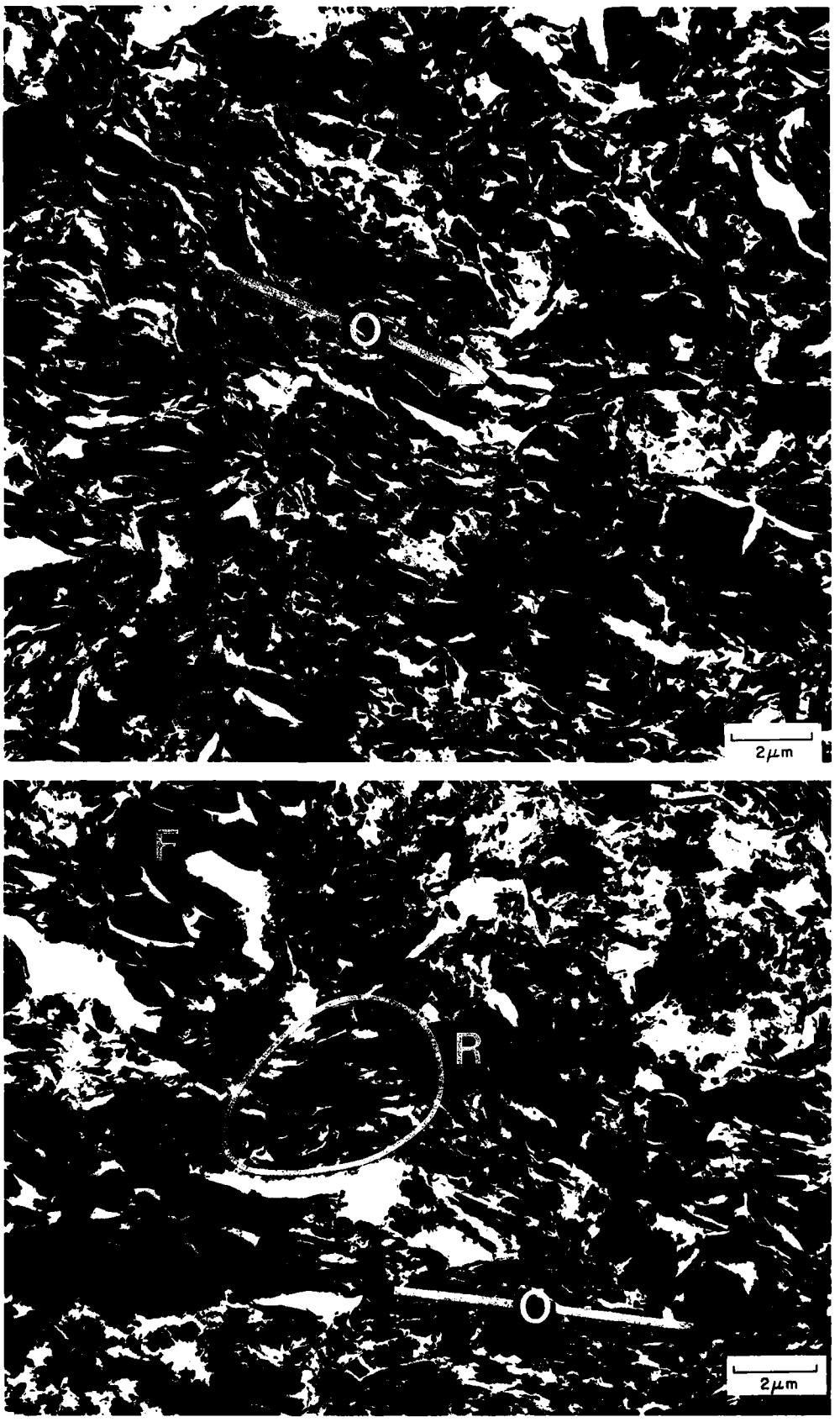

Figure 22.6(a,b). TEM photographs of Sample 671B-8H-4 (68.9 mbsf). Oriented with upcore direction at top of photographs. Porosity: 63%. Fairly open fabric of particle domains show zones of preferred orientation (O). Some possible packets of remolded (R) fabric surround fractillites (F).

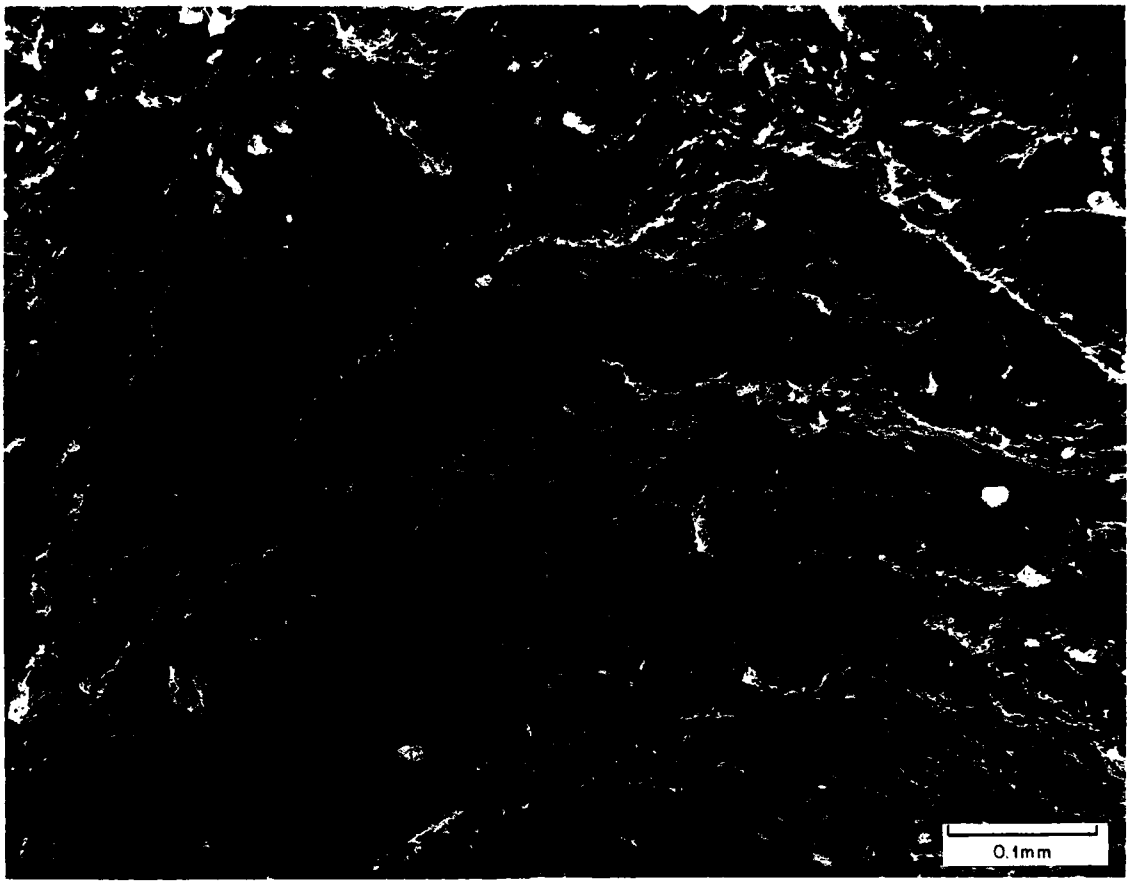

Figure 22.7. SEM photograph of Sample 671B-14X-4 (125.2 mbsf). Oriented with upcore direction at top of photograph. Porosity 58%. Sample from 3 m above the major thrust fault may reflect shear-related drag remolding of sediment fabric.

Localized remolding is suggested from swirled packets surrounding denser clays and fractillites. The lower porosity of this sample (63% compared to 76% for Sample 671B-2H-2) is associated with microfabric exhibiting local remolding and general development of a preferred orientation.

Sample 671B-14X-4 is located 2.8 m above the major thrust fault at 128 mbsf. The material in this sample represents the base of the uppermost thrust package. The porosity at the base of this package is nearly 50% compared to 72% porosity just below the fault. Figure 22.7 shows the relatively strong development of bedding parallel fabric with remolding possibly associated with near-field strain around the fault plane.

Sample 671B-28X-4 is from upper Pliocene calcareous mudstone lithologically equivalent to sediments sampled in Core 671B-8H. A major difference between these otherwise comparable samples is the much lower porosity of the deeper core: 50% instead of 60%. The lower porosity is evident in SEM and TEM images showing significantly less random fabric (Fig. 22.8). Zones of edge-to-edge aligned clay domains and particles are pervasive throughout this sample. The overall fabric within the oriented sample, however, does not appear to be preferentially aligned. Microshear planes form bent end-to-end chains. Lack of a general preferred orientation may account for no apparent fissility in these low porosity, calcareous mudstones.

Siliceous and smectitic mudstones of Unit II have a fine-grained, random, open fabric reflecting the porosities near 60% overlying the decollement (Fig. 22.9). The finer grain matrix does not exhibit dewatering channels or remolding evident in overlying sediments. The microfabric character of Sample 671B-45X-3 suggests little shear or compressive stress has altered this section of sediment.

Shear-related microstructural collapse of the open siliceous and smectitic mudstone fabric observed in Sample 671B-45X-4 takes place within, and below, the decollement. Sample 671B-56X-2, from the base of the decollement, has a very strongly oriented subhorizontal, bedding parallel fabric (Fig. 22.10). This type of fabric probably accounts for the scaly macrofabric described in visual core descriptions at this depth. The porosity loss through the 40-m-thick decollement is greater than 10% and accounts for the collapsed structure observed in this sample.

Figure 22.8. SEM photograph (a) and TEM photograph mosaic (b) of Sample 671B-28X-4 (257.6 mbsf). Oriented with upcore direction at top of photographs. Porosity: 50%. Lithologic equivalent to Sample 671B-8H but part of tectonic unit 2. Little evident visible deformation in the core is contrasted by end-to-end chains showing domains of moderate alignment. F, fractillite.

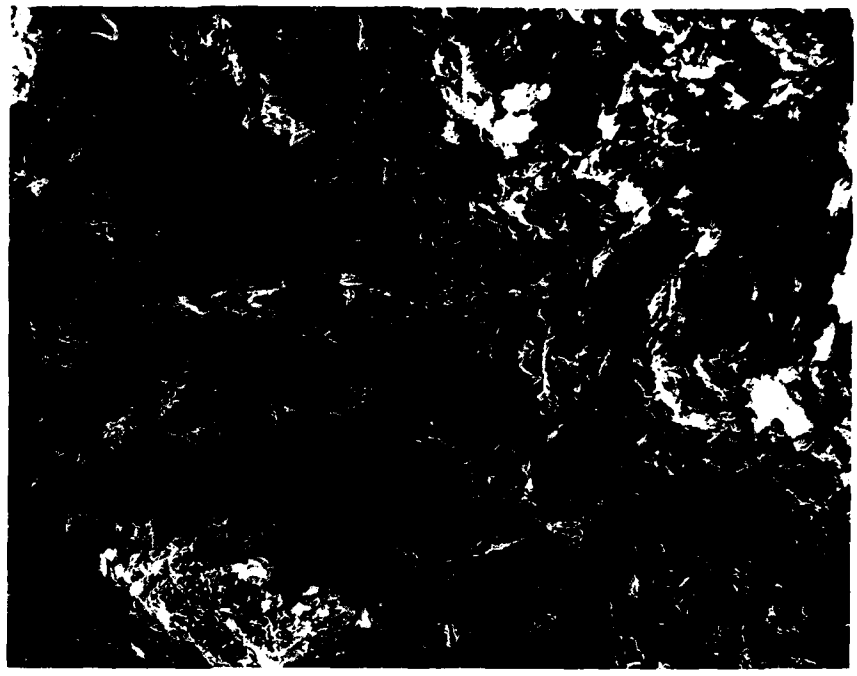

(a)

(b)

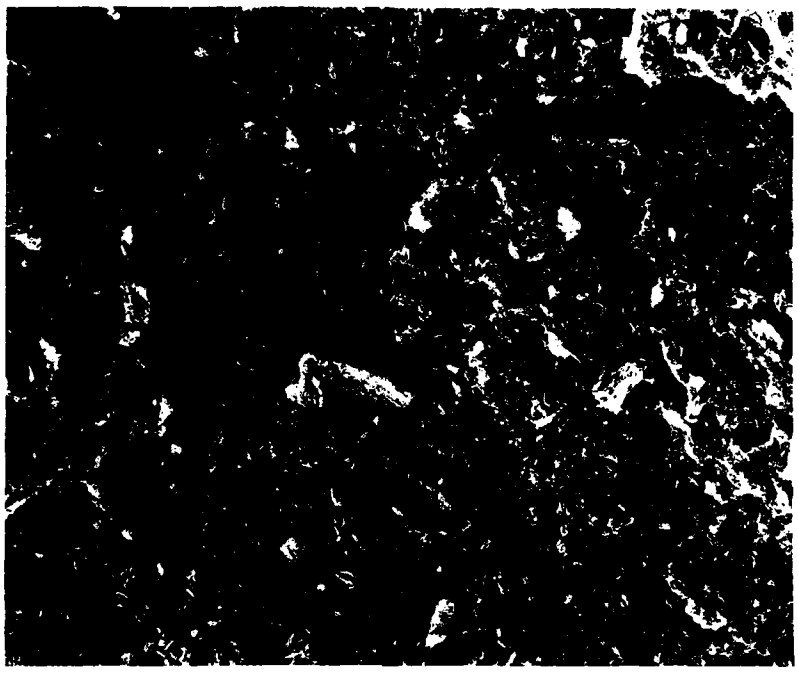

Figure 22.9. SEM photograph (a) and TEM photograph mosaic (b) of Sample 671B-45X-3 (410.0 mbsf). Only the SEM is oriented with the upcore direction at the top. Porosity:65%. Porous fabric composed of smectitic mudstone does not appear compacted under the corresponding overburden. B, nannofossil; F, fractillite; M, matrix.

Figure 22.9. (b)

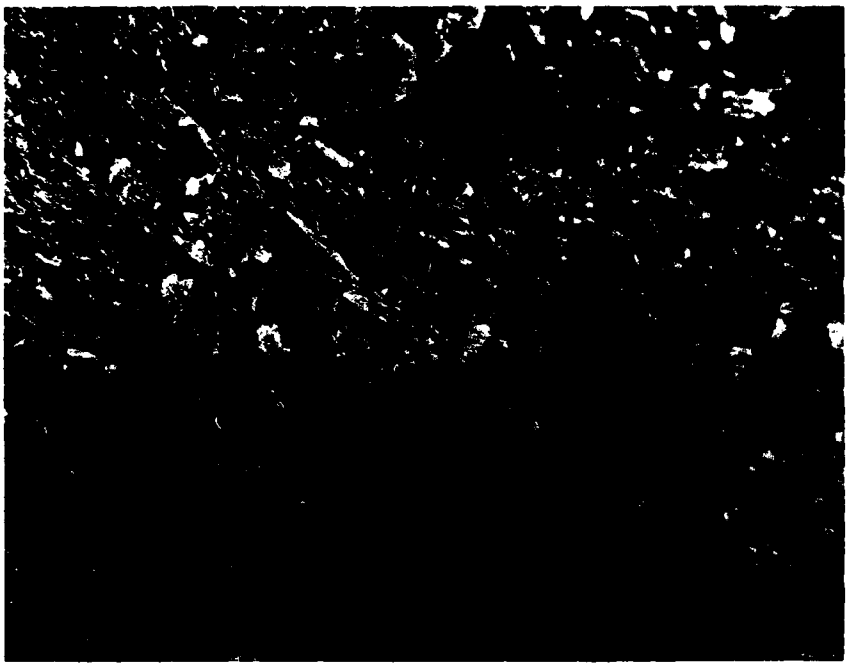

Figure 22.10(a,b). SEM photographs of Sample 671B-56X-2 (512.6 mbsf). Oriented with upcore direction at top of photographs. Porosity: 56%. Though retaining a relatively high porosity, sediments at the top of the decollement show evidence of preferred fabric orientation subparallel to bedding and shear direction.

Figure 22.11. SEM stereo-photograph of Sample 671B-61X-2 (560.0 mbsf). Oriented with upcore direction at top of photograph. Porosity: 50%. The base of the decollement shows sediment deformation following shear-related consolidation. Dense, subhorizontal fabric creates low intergranular permeabilities but brittle scaly cleavage results in higher formation permeability.

Progressive consolidation, dewatering, and hardening of this fine-grained mudstone are apparent as bedding-parallel clay packets develop into mudstone with brittle, subhorizontal scaly cleavage (Fig. 22.11).

Microfabric and Geotechnical Characteristics

Although comparison of sediment physical properties between Sites 671 and 672 suggests little evidence of lateral consolidation effects on accreted sediments, structural deformation within the offscraped section testifies to stresses on the column. Triaxial test results from sediments overlying the decollement indicate rotation of major and minor stress directions is associated with accretion (Moran and Christian, 1990). However, Site 672 and 671 sediments are progressively underconsolidated with depth suggesting *in situ* excess pore pressures. Despite the complex stress field there, a major control on the geotechnical character of the sediments near the Barbados deformation front seems to be lithologic composition.

Sediment microfabrics observed in SEM and TEM seem to substantiate the compositional control on sediment deformation. The offscraped calcareous mud(stone) is deformed within tectonic packages and near fault zones. These sediments develop zones of highly aligned chains, distributed in an apparently random fashion through the overall sample. The result of applied stresses in the accreted, calcareous mud(stone) is a decrease in porosity and permeability that closely follows that of nonaccreted equivalent facies at Site 672. Except for localized zones, the calcareous mud(stone) has developed little to no fissility. Localized zones of bedding-parallel, preferential particle alignment may be associated with thrust-fault strains.

High porosity, fine-grained siliceous and smectitic mudstones in offscraped sediments above, and forming, the decollement show an open, random fabric immediately above this major displacement plane. The low permeabilities of overlying calcareous mudstone may impede pore fluid migration, resulting in excess pore pressure build-up. The increase of pore pressure, in turn, reduces the strength of this sediment (Taylor and Leonard, 1990). Lower in the decollement, shear-induced strains have developed a strongly oriented microfabric in these same sediments leading to a pronounced porosity decrease within the 40-m-thick zone. The bedding-subparallel fabric results in greater fissility, which under stresses in the decollement may lead to development of scaly fabric. This scaliness in turn enhances bedding-parallel permeability allowing dewatering and structural collapse of the fabric (Moore et al., 1988). Continued consolidation and increasing strength lead to the scaly cleavage found in sediments below the decollement.

The calcareous mud(stone) and smectitic/siliceous mudstones recovered from the Barbados Forearc exhibit contrasting physical properties and structural deformation. Sediment composition appears to play a key role as a focus for the developing decollement at this active margin. The microstructural deformation observed within the Leg 110 sediments suggests significant small-scale disruption takes place during the early stages of accretion–subduction, despite the apparently limited reaction implied by the physical properties record.

References

American Society for Testing Materials, 1981. Annual Book of Standards, Part 19: Natural Building Stones, Soil and Rock. Philadelphia (ASTM).

Biju-Duval, B., J.C. Moore, et al., 1984. Initial Reports DSDP Volume 78A. U.S. Government Printing Office, Washington, D.C., 603 p.

Bray, C.J., and D.E. Karig, 1985. Porosity of sediments in accretionary prisms and some implications for dewatering processes. Journal of Geophysical Research, v. 90, p. 768-778.

Bray, C.J., and D.E. Karig, 1986. Physical properties of sediments from the Nankai Trough, Deep Sea Drilling Project Volume 87A, Sites 582 and 583. In: Kagami, H., D.E. Karig, et al. (eds.), Initial Reports DSDP Volume 87. United States Government Printing Office, Washington, D.C., p. 827-842.

Bryant, W.R., and R.H. Bennett, 1988. Origin, physical, and mineralogical nature of red clays: the Pacific Ocean basin as a model. Geo-Marine Letters, v. 8(8), p. 189-249.

Bryant, W.R., R.H. Bennett, and C.E. Katherman, 1981. Shear strength consolidation, porosity, and permeability of oceanic sediments. In: Emiliani, C. (ed.), The Oceanic Lithosphere: The Sea, v. 7. Wiley, New York, p. 1555-1616.

Burkett, P.J., 1987. Significance of the microstructure of Pacific red clays to nuclear waste disposal. M.S. Thesis, Texas A&M University, College Station, TX, 79 p.

Carson, B., 1977. Tectonic modification of deep-sea sediments at the Washington-Oregon continental margin: mechanical consolidation. Marine Geology, v. 24, p. 289-307.

Carson, B., and T.R. Bruns, 1980. Physical properties of sediments from the Japan Trench margin and outer trench slope: results from Deep Sea Drilling Project Leg 56 and 57. In: Scientific Party, Initial Reports DSDP Volumes 56 and 57, Part 2. United States Government Printing Office, Washington, D.C., p. 1187-1199.

Carson, B., and P.L. Berglund, 1986. Sediments deformation and dewatering under horizontal compression: experimental results. In: Moore, J.C. (ed.), Structural Fabrics in Deep Sea Drilling Project Cores from Forearcs. Geological Society of America Memoir 166, p. 135-150.

Carson, B., R. von Huene, and M. Arthur, 1982. Small-scale deformation structures and physical properties related to convergence in Japan Trench slope sediments. Tectonics, v. 1, p. 277-302.

Chiou, W.A., 1981. Clay fabric of gassy submarine sediments. Ph.D. dissertation, Texas A&M University, College Station, TX, 248 p.

Cowan, D.S., J.C. Moore, S.M. Roeske, N. Lundberg, and S.E. Lucas, 1984. Structural fabrics at the deformation front of the Barbados Ridge complex. Deep Sea Drilling Project Leg 78A. In: Biju-Duval, B., J.C. Moore, et al. (eds.), Initials Reports DSDP Volumes 78A and 78B. United States Government Printing Office, Washington, D.C., p. 535-548.

Hamilton, E.L., 1976. Variations of density and porosity with depth in deep sea sediments. Jour. Sed. Pet., 46(2):280-300.

Johns, M.W., 1986. Consolidation and permeability characteristics of Japan Trench and Nankai Trough sediments from DSDP Leg 87, Sites 582, 583, and 584. In: Kagami, H.D., E. Karig, et al. (eds.), Initial Reports DSDP Volume 87. United States Government Printing Office, Washington, D.C., p. 827-842.

Knipe, R.J., 1986. Microstructural evolution of vein arrays preserved in cores from the Japan Trench. In: Moore, J.C. (eds.), Structural Fabrics in Deep Sea Drilling Project Cores from Forearcs. Geological Society of America Memoir 166, p. 135-150.

Lambe, T.W., 1951. Soil Testing for Engineers. Wiley, New York, 165 p.

Lambe, T.W., and R.V. Whitman, 1969. Soil Mechanics. Wiley, New York, 553 p.

Lee, H.J., J.W. Olsen, and R. von Huene, 1973. Physical properties of deformed sediments from Site 181. In: Kulm, L.D., R. von Huene, et al. (eds.), Initial Reports DSDP Volume 18. United States Government Printing Office, Washington, D.C., p. 897-901.

Lowe, J., P.F. Zaccheo, and H.S. Feldman, 1964. Consolidation testing with back-pressure. Journal of Soil Mechanics and Foundations Division ASCE, v. 90, p. 69-86.

Lundberg, N., and J.C. Moore, 1986. Macroscopic structural features in Deep Sea Drilling Project cores from forearc regions. In: Moore, J.C. (ed.), Structural Fabrics in Deep Sea Drilling Project Cores from Forearcs. Geological Society of America Memoir 166, p. 13-44.

Marlow, M.S., H.J. Lee, and A.W. Wright, 1984. Physical properties of sediment from the Lesser Antilles margin along the Barbados Ridge: Result from DSDP Leg 78A. In: Biju-Duval, B., J.C. Moore, et al. (eds.), Initials Reports DSDP Volume 78A. United States Government Printing Office, Washington, D.C., p. 549-558.

Mascle, A., J.C. Moore, et al., 1988. Proceedings Ocean Drilling Program, Part A-Initial Results Volume 110. Ocean Drilling Program, College Station, TX., p. 603.

Moore, J.C., A. Mascle, et al., 1988. Tectonics and hydrogeology of the northern Barbados Ridge: results from Ocean Drilling Program Leg 110. Geological Society of America Bulletin, v. 100, p. 1578-1593.

Moran, K., and H.A. Christian, 1990. Strength and deformation behavior of sediment from the Lesser Antilles forearc accretionary prism. In: Moore, J.C., A. Mascle, et al. (eds.), Proceedings of the Ocean Drilling Program Scientific Results, Volume 110. Ocean Drilling Program, College Station, TX., p. 279-288.

Shephard, L.D., and W.R. Bryant, 1980. Consolidation characteristics of Japan Trench sediments. In: Scientific Party Initial Reports DSDP Volumes 56 and 57, Part 2. United States Government Printing Office, Washington, D.C., p. 279-312.

Shephard, L.E., W.R. Bryant, and W.A. Chiou, 1980. Geotechnical properties of Middle America Trench sediments, Deep Sea Drilling Project Leg 66. In: Watkins, J.S., J.C. Moore, et al. (eds.), Initial Reports DSDP volume 66. United States Government Printing Office, Washington, D.C., p. 475-504.

Shephard, L.E., and W.R. Bryant, 1983. Geotechnical properties of lower trench inner slope sediments. Tectonophysics, 279-312.

Suess, E., R. von Huene, et al., 1988. Proceedings of the Ocean Drilling Program, Initial Reports, Volume 112. Ocean Drilling Program, College Station, TX., 1015 p.

Taylor, E., and W.R. Bryant, 1985. Geotechnical properties of sediments from the Middle America trench and slope. In: von Huene, R., J. Aubouin, et al. (eds.), Initial Reports DSDP Volume 84. United States Government Printing Office, Washington, D.C., p. 551-570.

Taylor, E., and J.N. Leonard, 1990. Sediment consolidation and permeability at the Barbados forearc. In: Moore, J.C., A. Mascle, et al. (eds.), Proceedings of the Ocean Drilling Program, Scientific Results Volume 110. Ocean Drilling Program, College Station, TX., p. 289-308.

Wackler, J.D., 1988. Microstructures and fabrics of sediments from the lesser Antilles accretionary complex. M.S. Thesis, Texas A&M University, College Station, TX, 159 p.